Engineering Chemistry
ISSN: 2813-6535, Vol. 3, pp 37-43
doi:10.4028/p-497n8w

Submitted: 2023-02-23
Accepted: 2023-03-12
Online: 2023-06-20

Chemical and Morphological Analysis of Calcium Oxide (CaO) Powder from Sea Urchin (Diadema setosum) Shell

Muhammad Amir Jamilludin[1,a], I Kadek Hariscandra Dinatha[1,b], Apri I. Supii[2,c], Juliasih Partini[1,d], Dwi Liliek Kusindarta[3,e] and Yusril Yusuf[1,f,*]

[1]Department of Physics, Faculty of Mathematics and Natural Science, Gadjah Mada University, Indonesia

[2]Research Centre for Marine and Bioindustry, National Research and Innovation Agency, Indonesia

[3]Department of Anatomy, Faculty of Veterinary Medicine, Gadjah Mada University, Indonesia

[a]muhammadamirjamilludin@mail.ugm.ac.id, [b]ikadekhariscandradinatha@mail.ugm.ac.id, [c]aprisupii@yahoo.co.id, [d]juliasih@ugm.ac.id, [e]indarta@ugm.ac.id, [f]yusril@ugm.ac.id

Keywords: Calcination, calcium carbonate, calcium oxide, sea urchin shell.

Abstract. Calcium carbonate ($CaCO_3$) has been taken from sea urchin (*Diadema setosum*) shell and calcinated at several temperatures to obtain calcium oxide (CaO). X-Ray Fluorescence Spectroscopy (XRF) revealed that the powder from this shell had a high Ca level, which increased at a higher temperature. Fourier Transform Infrared Spectroscopy (FTIR) spectra agreed to an increase in Ca level that showed the presence of CaO at 900 ºC and 1100 ºC; otherwise, $CaCO_3$ disappeared. Using Scanning Electron Microscopy (SEM), the powder morphology was more homogeneous at 900 ºC and 1100 ºC than at lower temperatures. This morphology was encouraged by decreasing particle size, indicating compound decomposition in the powder and Ca leaved. This decomposition was confirmed by an Energy Dispersive X-ray Spectroscopy (EDS) analysis that showed increased Ca content with higher mass and atomic level at a higher temperature.

Introduction

Sea urchin (*Diadema setosum*) shell is the source of Ca in the form of calcium carbonate ($CaCO_3$), which highly potential for synthesizing CHAp[1], like other natural shells such as common cockle shell[2], cockle shell[3], and oyster shell[4] with high of Ca level. Calcium (Ca) contribute to several functions in the human body[5]. Ca can be used for biomedical purposes, even several environmental technologies[6,7]. In other applications, $CaCO_3$ is decomposed into calcium oxide (CaO), which shows potential as biomaterials for bone and teeth implants[8]. Transforming $CaCO_3$ into CaO needed a calcination process with calcination temperature that depended on the nature of the compounds before the shell was calcinated[9]. In the previous study, the abalone mussel shell had a Ca level of 33.58% before calcination at 1000 ºC, and the Ca level increased up to 56.32%[10]. In another study, green mussel shell has been reported Ca level 30.43% at calcination temperature 600 ºC, then increase until 49.58% at 950 ºC which higher and potential as a precursor for hydroxyapatite synthesis, at this calcination temperature indicated breaking of chemical bond of $CaCO_3$ into CaO is faster, confirmed by infrared spectra analysis[11]. Calcination temperature can affect the characteristics and phase transition of CaO[9]. Previous research has studied the effect of calcination temperature at 850 ºC for aquatic materials, including oyster shells, mussel shells, and cuttlebone, and obtained optimum material conditions[12]. Another study reported that crab shell was calcinated at a temperature of 700 ºC and obtained appropriate material for synthesizing hydroxyapatite[13]. In this study, sea urchin shell was used as raw materials. We analyzed the effects of calcination temperature on the powder's chemical and morphological characteristics derived from the shell.

Materials and Methods

Synthesis of CaO Powder. Sea urchin shells were taken from Bali. The shells were washed with distilled water and boiled for 30 minutes, then sun-dried for 8 hours. The shells were soaked in acetone for 24 hours and then sun-dried for 6 hours. As dried, to obtain $CaCO_3$ powder, the shells were milled for 30 seconds in 3 times repetition. The powder was calcined in a furnace for 6 hours with temperature variations of 600 ºC, 800 ºC, 900 ºC, and 1100 ºC to obtain pure CaO.

Characterization of CaO Powder. The chemical composition of powders was characterized by X-Rays Fluorescence (XRF [RIGAKU-NEX + QuanTEZ]), including atomic level. The functional group of powders were characterized by FTIR (Thermo Nicolet iS10, Japan); this FTIR characterization used a range of wavenumber 650-4000 cm^{-1}. The morphology of powders was observed using Scanning Electron Microscopy (SEM, Joel JSM-6510LA-1400, Japan) with an accelerating voltage of 15 kV and magnification of 1000 times. Powders' particle size distribution was calculated using ImageJ by measuring 60 random particles. To determine the composition of calcium and other compounds in powders, used Energy Dispersive X-ray Spectroscopy (EDS) that included while performing SEM.

Results and Discussions

The Ca level of the powders was characterized using XRF. As shown in Table 1, calcinated powder at 900 ºC and 1100 ºC had the highest Ca level; with the same value. Ca level significantly increased when calcination temperature increased, but at 1100 ºC, the increase became slow. Fig. 1(a)-(d) shows that the powders had an increasing intensity of Ca-Kα while calcination temperature increased, which confirmed the increase in Ca level. As shown in Fig. 1(a) and (b), the intensity of the Ca-Kα peak slightly increased. As in Fig. 1(c) and (d), the increase in Ca-Kα intensity peak was significant compared with lower temperature. Sr impurity remained at a superficial level in all temperatures, not more than 1,2%.

Table 1. Percentage of Ca level.

Powder at variation of calcination temperature	Ca level (%)
600 ºC	93.39 ± 0.10
800 ºC	94.79 ± 0.05
900 ºC	96.01 ± 0.02
1100 ºC	96.06 ± 0.02

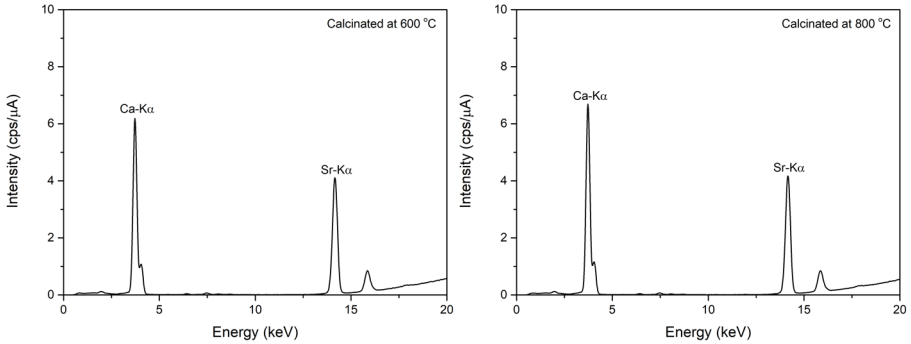

(a) (b)

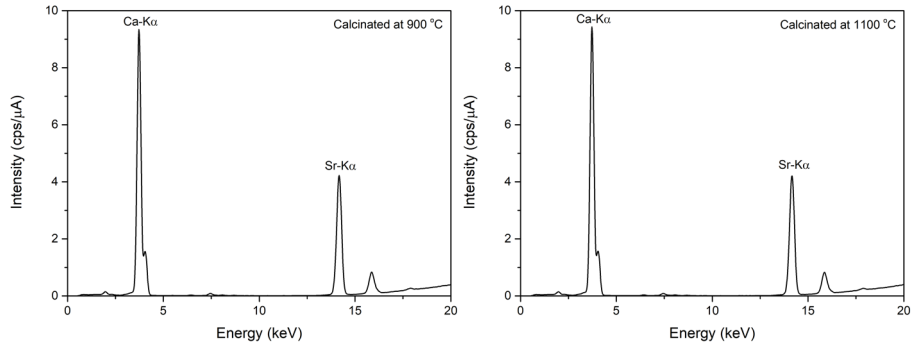

(c) (d)

Figure 1. XRF spectra of calcinated powders at (a) 600 ºC, (b) 800 ºC, (c) 900 ºC, and (d) 1100 ºC.

Fig. 2 shows FTIR spectra of the powders. It is shown in Fig. 2(a) and (b) that calcinated powder at 600 ºC and 800 ºC had a bond functional group of C-O and C=O at the same position, C-O bond at 713.53 cm^{-1}, 871.67 cm^{-1}, and 1396.21 cm^{-1}, and C=O bond at 1795.40 cm^{-1}, indicated the presence of $CaCO_3$. The positions of the C-O bond functional group were close to references of the C-O bond functional group[14,15]. The transmittance of C-O and C=O bonds increased while calcination temperature increased, which meant the $CaCO_3$ level decreased. The C=O bond disappeared, then another C=O bond appeared at 2049.96 cm^{-1} at 900 ºC, and the transmittance became lower at 1100 ºC. OH- stretching functional group appeared for the first time at 3639.98 cm^{-1} at calcination temperature 800 ºC, and transmittance became lower at higher calcination temperature, which confirmed the increase of CaO level according to the OH group. CaO bond functional group was present at 874.56 cm^{-1} at 900 ºC, and the transmittance became lower at 1100 ºC, which meant the CaO level increased. The increase in CaO was not significant; this could be seen in Fig. 2(c) and (d).

This result concluded that $CaCO_3$ was decomposed into CaO triggered by the calcination process, with 900 ºC as the minimum temperature for the decomposition process[10]. $CaCO_3$ received heat, causing atoms to move faster. This condition led breaking process of the $CaCO_3$ chemical bond into CaO and CO_2; at higher calcination temperature chemical bond is broken more quickly[11,16,17].

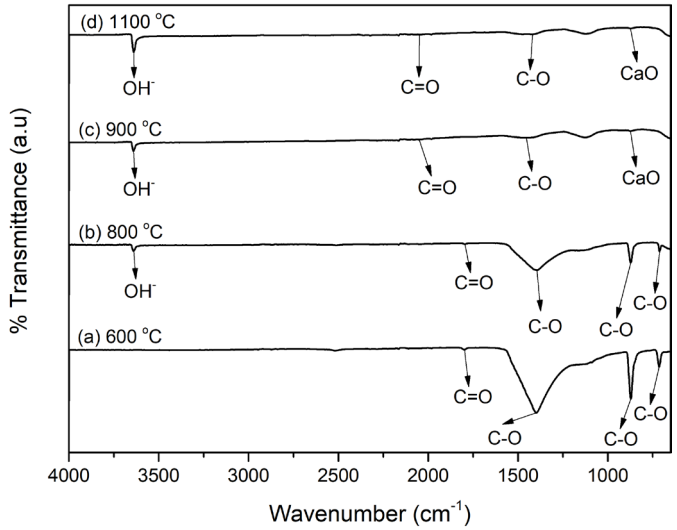

Figure 2. FTIR spectra of calcinated powders at (a) 600 ºC, (b) 800 ºC, (c) 900 ºC, and (d) 1100 ºC.

Fig. 3(a1,a2)-(d1,d2) shows the powders' morphology and particle size distribution characterized using SEM. It is shown that calcinated powder at higher temperatures caused smaller particle sizes. As shown in Fig. 3(a1,a2), the particle distribution was heterogeneous at 600 ºC, and the particle size was large, about 8.10 μm. Fig. 3(b1,b2) shows that particles had been reduced into smaller particles size of 7.28 μm but remained with irregular and ununiform shapes at 800 ºC. As seen in Fig. 3(c1,c2)-(d1,d2), the particles quickly became homogeneous and orderly distributed at higher calcination temperatures, at 900 ºC and 1100 ºC, with smaller particle sizes up to 4.78 μm. But at those

temperatures, the particles had interconnected and agglomerated shapes in a solid structure, indicating optimum calcination temperatures. This particle size reduction defined particle compounds' decomposition at the atomic level, indicating that the calcination process released CO_2 and created cavities[10]. It could be seen at 1100 ºC; cavities created are more than 900 ºC. In those temperatures, the distribution and size of particles were almost the same or slight differed compared with lower temperatures.

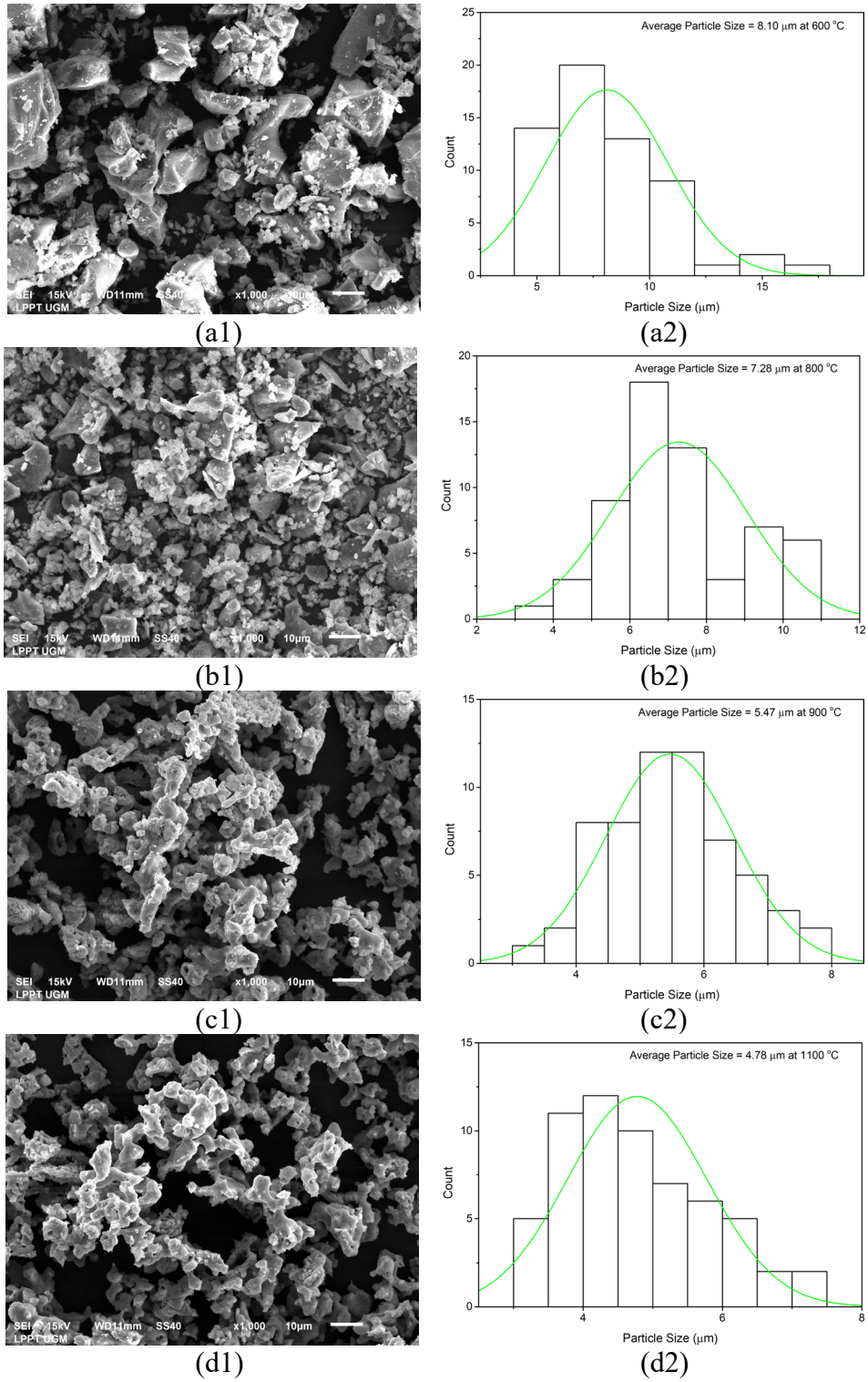

Figure 3. SEM analysis of calcinated powders at (a1,a2) 600 ºC, (b1,b2) 800 ºC, (c1,c2) 900 ºC, and (d1,d2) 1100 ºC.

Fig. 4 show the EDS spectra of the powders. It is shown in Fig. 4(a)-(d) that at higher calcination temperatures, CaKα and CaKβ had a higher peak, which meant the Ca level was increasing. The mass and atom count percentage of Ca obtained during characterization was performed in Table 2, which shows an increasing value which confirms the decomposition process of another compound and leaves Ca caused decreasing in particle size in SEM analysis. While the temperature was raised, decomposition occurred faster; this heat helped optimize decomposition[18]. At 900 ºC and 1100 ºC, the increase of Ca was low, indicating a slower decomposition process.

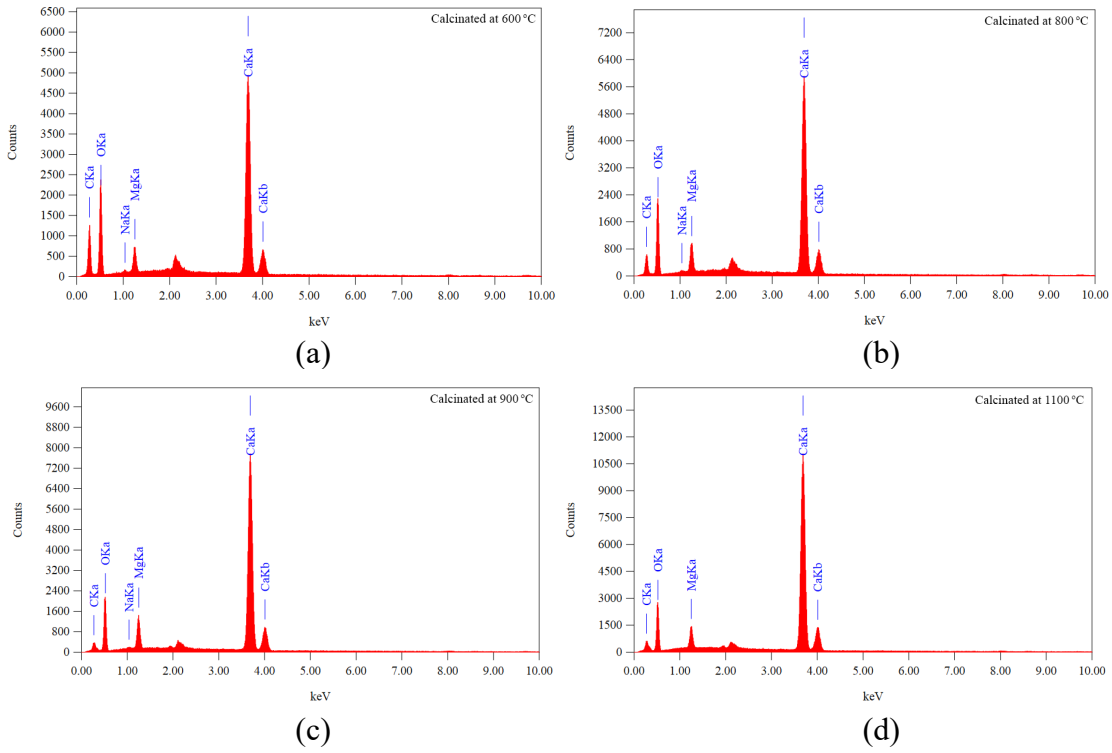

Figure 4. EDS analysis of calcinated powders at (a) 600 ºC, (b) 800 ºC, (c) 900 ºC, and (d) 1100 ºC.

Table 2. Percentage of Ca mass and atom.

Powder at variation of calcination temperature	Ca mass (%)	Ca atom (%)
600 ºC	36.07	17.57
800 ºC	41.37	21.66
900 ºC	48.31	27.40
1100 ºC	50.63	29.05

Conclusions

In this experiment, CaO was synthesized from sea urchin shells through calcination. The XRF analysis showed the powder had the highest Ca level, up to 96% at 900 ºC and 1100 ºC. FTIR results revealed changes in functional groups indicated phase transition from $CaCO_3$ into CaO, CaO was present for the first time at 900 ºC, and Ca level became higher at 1100 ºC. The infrared spectra showed that 900 ºC was possibly being minimum calcination temperature for CaO appearance through the decomposition process. SEM results showed particle distribution became more homogeneous and orderly distributed in higher calcination temperatures with smaller particle sizes, indicating the decomposition of powder leaving Ca content. This SEM analysis was confirmed by the EDS result that showed the percentage of Ca increased while calcination temperature increased. From all those analysis results, increasing Ca was fast until 900 ºC and became slow when it reached 1100 ºC. This high Ca content encourages the possibility for biomaterial application, certainly in the synthesis of hydroxyapatite (HAp) or carbonated hydroxyapatite (CHAp).

Acknowledgement

The authors thank PMDSU scholarship for financial support in this research and the Ministry of Education and Culture Republic of Indonesia for the grant (1995/UNI/DITLIT/Dit-Lit/PT.01.03/2022), also Research Centre for Marine and Bioindustry for sea urchin resource. The authors acknowledge been worked with technical assistance and using research instruments and testing facilities of the Laboratory for Research and Testing Universitas Gadjah Mada, Indonesia.

References

[1] I. K. Januariyasa and Y. Yusuf, "Porous carbonated hydroxyapatite-based scaffold using simple gas foaming method," Journal of Asian Ceramic Societies, vol. 8, no. 3, pp. 634–641, Jul. 2020, doi: 10.1080/21870764.2020.1770938.

[2] A. Aminatun *et al.*, "Biopolymer-based polycaprolactone-hydroxyapatite scaffolds for bone tissue engineering," *International Journal of Polymeric Materials and Polymeric Biomaterials*, 2021, doi: 10.1080/00914037.2021.2018315.

[3] Y. Rizkayanti and Y. Yusuf, "Effect of Temperature on Synthesis of Hydroxyapatite from Cockle Shells (Anadara Granosa)," 2018.

[4] Almukarrama and Y. Yusuf, "Development Carbonated Hydroxyapatite Powders from Oyster Shells (Crassostrea gigas) by Sintering Time Controlling," in *IOP Conference Series: Materials Science and Engineering*, Jul. 2019, vol. 546, no. 4. doi: 10.1088/1757-899X/546/4/042001.

[5] G. Cormick and J. M. Belizán, "Calcium intake and health," *Nutrients*, vol. 11, no. 7. MDPI AG, Jul. 01, 2019. doi: 10.3390/nu11071606.

[6] P. Terzioğlu, H. Öğüt, and A. Kalemtaş, "Natural calcium phosphates from fish bones and their potential biomedical applications," *Materials Science and Engineering C*, vol. 91. Elsevier Ltd, pp. 899–911, Oct. 01, 2018. doi: 10.1016/j.msec.2018.06.010.

[7] J. A. Currie, N. R. Harrison, L. Wang, M. I. Jones, and M. S. Brooks, "A preliminary study of processing seafood shells for eutrophication control," *Asia-Pacific Journal of Chemical Engineering*, vol. 2, no. 5, pp. 460–467, Sep. 2007, doi: 10.1002/apj.82.

[8] V. K. Mishra, S. K. Srivastava, B. P. Asthana, and D. Kumar, "Structural and Spectroscopic Studies of Hydroxyapatite Nanorods Formed via Microwave-Assisted Synthesis Route," *Journal of the American Ceramic Society*, vol. 95, no. 9, pp. 2709–2715, Sep. 2012, doi: 10.1111/j.1551-2916.2012.05134.x.

[9] N. Suwannasingha, A. Kantavong, S. Tunkijjanukij, C. Aenglong, H. B. Liu, and W. Klaypradit, "Effect of calcination temperature on structure and characteristics of calcium oxide powder derived from marine shell waste," *Journal of Saudi Chemical Society*, vol. 26, no. 2, Mar. 2022, doi: 10.1016/j.jscs.2022.101441.

[10] M. Sari, P. Hening, Chotimah, I. D. Ana, and Y. Yusuf, "Porous structure of bioceramics carbonated hydroxyapatite-based honeycomb scaffold for bone tissue engineering," *Materials Today Communications*, vol. 26, Mar. 2021, doi: 10.1016/j.mtcomm.2021.102135.

[11] M. Sari and Y. Yusuf, "Synthesis and characterization of hydroxyapatite based on green mussel shells (perna viridis) with the variation of stirring time using the precipitation method," in *IOP Conference Series: Materials Science and Engineering*, Nov. 2018, vol. 432, no. 1. doi: 10.1088/1757-899X/432/1/012046.

[12] S. Soisuwan, J. Phommachant, W. Wisaijorn, and P. Praserthdam, "The Characteristics of Green Calcium Oxide Derived from Aquatic Materials," *Procedia Chemistry*, vol. 9, pp. 53–61, 2014, doi: 10.1016/j.proche.2014.05.007.

[13] B. N. Bhattacharjee, V. K. Mishra, S. B. Rai, O. Parkash, and D. Kumar, “Structure of Apatite Nanoparticles Derived from Marine Animal (Crab) Shells: An Environment-Friendly and Cost-Effective Novel Approach to Recycle Seafood Waste,” *ACS Omega*, vol. 4, no. 7, pp. 12753–12758, Jul. 2019, doi: 10.1021/acsomega.9b00134.

[14] S. Rujitanapanich, P. Kumpapan, and P. Wanjanoi, “Synthesis of hydroxyapatite from oyster shell via precipitation,” in *Energy Procedia*, 2014, vol. 56, no. C, pp. 112–117. doi: 10.1016/j.egypro.2014.07.138.

[15] J. H. Shariffuddin, M. I. Jones, and D. A. Patterson, “Greener photocatalysts: Hydroxyapatite derived from waste mussel shells for the photocatalytic degradation of a model azo dye wastewater,” *Chemical Engineering Research and Design*, vol. 91, no. 9, pp. 1693–1704, Sep. 2013, doi: 10.1016/j.cherd.2013.04.018.

[16] M. Sari, P. Hening, Chotimah, I. D. Ana, and Y. Yusuf, “Bioceramic hydroxyapatite-based scaffold with a porous structure using honeycomb as a natural polymeric Porogen for bone tissue engineering,” *Biomaterials Research*, vol. 25, no. 1, Dec. 2021, doi: 10.1186/s40824-021-00203-z.

[17] H. A. Permatasari and Y. Yusuf, "Characteristics of Carbonated Hydroxyapatite Based on Abalone Mussel Shells (Halioitis asinina) Synthesized by Precipitation Method with Aging Time Variations," in *IOP Conference Series: Materials Science and Engineering*, Jul. 2019, vol. 546, no. 4. doi: 10.1088/1757-899X/546/4/042031.

[18] M. Sari and Y. Yusuf, "Synthesis and Characterization of Hydroxyapatite based on Green Mussel Shells (Perna viridis) with Calcination Temperature Variation Using the Precipitation Method," 2018.